



## Treatment of rounded and sharp corners in the numerical modeling of 2D electrostatic fields

Laurent Krähenbühl, François Buret, Ronan Perrussel, Damien Voyer, Patrick Dular, Victor Péron, Clair Poignard

### ► To cite this version:

Laurent Krähenbühl, François Buret, Ronan Perrussel, Damien Voyer, Patrick Dular, et al.. Treatment of rounded and sharp corners in the numerical modeling of 2D electrostatic fields. MOMAG, Aug 2010, Vitória, Brazil. pp.CD. hal-00502238v4

**HAL Id: hal-00502238**

**<https://hal.science/hal-00502238v4>**

Submitted on 2 Sep 2010

**HAL** is a multi-disciplinary open access archive for the deposit and dissemination of scientific research documents, whether they are published or not. The documents may come from teaching and research institutions in France or abroad, or from public or private research centers.

L'archive ouverte pluridisciplinaire **HAL**, est destinée au dépôt et à la diffusion de documents scientifiques de niveau recherche, publiés ou non, émanant des établissements d'enseignement et de recherche français ou étrangers, des laboratoires publics ou privés.

# Numerical treatment of rounded and sharp corners in the modeling of 2D electrostatic fields

L. Krähenbühl, F. Buret, R. Perrussel, D. Voyer  
Laboratoire Ampère (CNRS UMR5005)  
Université de Lyon, École Centrale de Lyon, France  
e-mail: laurent.krahenbuhl@ec-lyon.fr

P. Dular  
F.R.S.-FNRS, ACE research-unit  
Université de Liège, Belgium  
e-mail: patrick.dular@ulg.ac.be

V. Péron, C. Poignard  
INRIA, MC2 team-project  
Université de Bordeaux, France  
e-mail: clair.poignard@inria.fr

**Abstract**—This work deals with numerical techniques to compute electrostatic fields in devices with rounded corners in 2D situations. The approach leads to the solution of two problems: one on the device where rounded corners are replaced by sharp corners and the other on an unbounded domain representing the shape of the rounded corner after an appropriate rescaling. Details are given on several ways to solve both problems and numerical results are provided to assess the efficiency and the accuracy of the techniques.

## I. INTRODUCTION

The precise description of an object containing *rounded corners* leads to consider meshes with a large number of nodes when the finite element method (FEM) is straightforwardly applied. Dealing with such meshes makes the computation time- and resource-consuming. Moreover, these computations have to be repeated if the curvature radius of the rounded corner is modified.

In order to avoid this computational cost, the rounded corners are usually replaced by *sharp corners*. The obtained computational results are then “globally correct” but locally inaccurate in the neighborhood of the corners. We aim at remedying this drawback.

In this work, we are dealing with a 2D electrostatic problem in a domain with a rounded corner (see Fig. 1(a)). The proposed method to approximate the electric scalar potential is based on two observations, which can be checked by simple numerical experiments:

- the exact solutions *close to the corner*, computed for several values of the curvature radius  $\varepsilon$ , are quasi-similar, up to a “scaling factor” (related to  $\varepsilon$ ). It is also noticed that the “shape” of the solutions *close to the corner* (their “shape” but not their amplitude) weakly depend on other elements of the studied structure, such as the distance to the boundaries: it is said that the dominant term of the solutions close to the corner are *self-similar*.
- the exact solutions *far from the corner* are weakly influenced by the change of the curvature radius  $\varepsilon$ , and they converge to the solution on the domain with the sharp corner when  $\varepsilon$  goes to zero.

It can be deduced that an accurate approximate solution of the exact solution for any curvature radius  $\varepsilon$  can be build from the solutions of two problems:

- an electrostatic problem on the real domain except that the rounded corner is replaced by a sharp corner;
- an electrostatic problem on a domain that only takes the shape of the rounded corner into account. The corresponding solution will be used with an appropriate “scaling”.

This intuitive argument coincides with the mathematical results proposed partially by Timouyas [1] in 2003 and recently completed by Dauge and her collaborators [2]. In addition to the predictable behavior of the solution, some error estimates are also provided in [1], [2] for the approximate solutions we consider.

This work is addressed to the community of engineers that use numerical methods (as it was done in [3]), and the aim is to illustrate the finite element implementation of the theoretical concepts which are proved in other references [4], [2].

In Section II are given the principles of the method. Then, we provide explicitly how to solve the different problems, that enable to build the approximate solution:

- the computation of the “singularity factor” of the solution on the domain with the sharp angle, in Section III;
- the problem on the unbounded domain taking only into account the shape of the rounded corner, in Section IV.

In Sections II, III and IV, numerical results are given to assess the accuracy of the proposed techniques.

## II. PRINCIPLES OF THE METHOD

For the sake of clarity, the method is explained on a specific structure, see Fig. 1, but it can be straightforwardly extended to other structures, in particular including more than two electric conductors.

### A. Definitions of the considered problems

Denote by  $v_\varepsilon$  the harmonic function  $-\Delta v_\varepsilon = 0$  in the domain  $\Omega_\varepsilon$  equal to zero on  $\Gamma_\varepsilon^0$ , to  $V^1$  on  $\Gamma^1$  and satisfying homogeneous Neumann conditions on  $\Gamma^N$ ; see Fig.1(a). The factor  $\varepsilon$  defines the true size of the rounded corner, starting from the profile domain, Fig. 1(c) where the characteristic size of the rounded corner is 1.

Let also  $v$  denote the solution of  $\Delta v = 0$  in the domain  $\Omega$  with the sharp corner, see Fig. 1(b). The function  $v$  is enforced to be equal to zero on  $\Gamma^0$  and to  $V^1$  on  $\Gamma^1$ , and  $v$  verifies homogeneous Neumann conditions on  $\Gamma^N$ . In the

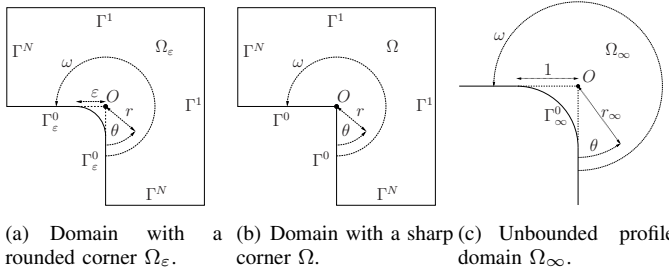


Fig. 1. Considered domains  $\Omega$ ,  $\Omega_\infty$  and  $\Omega_\epsilon$ .

neighborhood of the sharp corner<sup>1</sup>,  $v$  can be expanded in series as follows [5]:

$$v(r, \theta) = \lambda r^\alpha \sin(\alpha\theta) + \sum_{k=2}^{\infty} a_k r^{k\alpha} \sin(k\alpha\theta), \quad \left(\alpha = \frac{\pi}{\omega}\right), \quad (1)$$

and the first term of this expansion is said singular because it makes the amplitude of the electric field go to the infinite at the sharp corner for  $\alpha < 1$ . The factor  $\lambda$  is called the *singularity factor* in the following. Methods for the computation of  $\lambda$  are given in Section III. A specific notation will also be used for the first function of expansion (1):

$$S(r, \theta) = r^\alpha \sin(\alpha\theta). \quad (2)$$

Finally, let  $v_\infty$  denote the solution of  $\Delta v_\infty = 0$  in the unbounded domain  $\Omega_\infty$  where the characteristic size of the rounded corner is 1, see Fig. 1(c). The rounded corner has the same shape as in the real domain  $\Omega_\epsilon$ , the potential is zero on  $\Gamma_\infty^0$ , and the behavior of the potential at infinity is given by the first term of the expansion (1) up to the scalar  $\lambda$ :

$$\lim_{r_\infty \rightarrow \infty} (v_\infty(r_\infty, \theta) - S(r_\infty, \theta)) = 0. \quad (3)$$

The FEM enables to compute the term  $v_\infty$  whatever rounded corner shape (see Section IV). Note that for particular shapes analytic expressions of  $v_\infty$  can be obtained, for instance using conformal maps.

It is assumed in the remainder of this section that the approximate finite element solutions for  $v$  and  $v_\infty$  have already been computed.

### B. Proposed approximate solution

Solution  $v_\epsilon$  can be computed by the FEM, using a “fine” discretization close to the rounded corner. However, this computation has to be performed for each corner “scale”  $\epsilon$ .

Our aim is to approximate the solution  $v_\epsilon$  by using only:

- the solution  $v$ , that will approximate  $v_\epsilon$  far from the corner, i.e. when  $r \gg \epsilon$ ;
- the solution  $v_\infty$ , after a proper scaling by  $\epsilon$  and the singularity coefficient  $\lambda$ , that will approximate the solution close to the corner, i.e. when  $r \leq \epsilon$ .

<sup>1</sup>It is valid on any intersection of a disc centered in  $O$  with the domain  $\Omega$  which coincides with the intersection of the same disc with an infinite sector whose corner is in  $O$  and whose angle is  $\omega$ .

The “scaling” used to map a point of coordinate  $(r, \theta)$  in  $\Omega_\epsilon$  to a point in  $\Omega_\infty$  is given by  $(r_\infty, \theta) = (r/\epsilon, \theta)$ . This change of coordinates applied in (2) leads to:

$$\epsilon^\alpha S(r_\infty, \theta) = S(r, \theta). \quad (4)$$

These considerations enable to understand the following approximate expressions, that are detailed in [2]:

$$v_\epsilon(r, \theta) \approx \lambda \epsilon^\alpha v_\infty(r_\infty, \theta), \quad \text{for } r < k\epsilon \text{ (usually, } k = 1), \quad (5)$$

$$v_\epsilon(r, \theta) \approx v(r, \theta) + \lambda \epsilon^\alpha [v_\infty(r_\infty, \theta) - S(r_\infty, \theta)], \quad (6)$$

for  $r > k\epsilon$ .

### C. Remarks

The proposed expressions remain approximate, indeed:

- expressions (5) and (6) are not equal for  $r = k\epsilon$ , in particular when the geometry of the domain  $\Omega_\epsilon$  makes the solution for  $r < k\epsilon$  to be not symmetric (in this first order approximation, the effect of the domain  $\Omega_\epsilon$  close to the corner is only related to the value of the singularity factor  $\lambda$ . It is not sufficient: every problem with the same angle  $\omega$  and the same  $\lambda$  will give the same approximate solution close to the corner).
- in (6),  $(v_\infty(r_\infty, \theta) - S(r_\infty, \theta))$  is not exactly zero on  $\Gamma_\infty^1$ : thus, the conditions on this boundary, which are satisfied by  $v$ , are not satisfied by approximation (6). However, it can be seen, that whenever  $\epsilon$  goes to zero, the remaining error becomes negligible: the scaling of the domain makes to send the boundaries further from the origin in the dimensionless solution  $v_\infty$  and the behavior at infinity (3) can be used.

It is possible to compute complementary terms, to increase the accuracy of the approximate solution. In particular, the following term in the expansion, which will vary as  $\sin(2\alpha\theta)$  (it comes from (1)), will be able to introduce an asymmetry of the approximation close to the rounded corner. Nonetheless, our numerical experiments with the first terms of the expansion show the relevance of this first order approach and illustrate the theoretical estimates for the numerical error [2].

We emphasize that the method is generic and could be applied to other particular shapes which would not be “rounded” (and even to a simple surface irregularity, on a surface plane).

### D. Application to the computation of the maximum field as a function of the curvature radius

With a reduced amount of numerical computations, a mesh without the rounded corner of the whole studied device and a mesh of the rounded corner but built independently from the rest of the structure, it is possible to determine the variation of the electric field close to the rounded corner as a function of the curvature radius. Indeed, the electric field  $E_\epsilon(r, \theta)$  in any point close to the rounded corner depends only on:

- the singularity factor  $\lambda$  whose evaluation is introduced in Section III starting from  $v$  the solution with the sharp corner;
- the field  $E_\infty(r_\infty, \theta)$  transferred to the domain  $\Omega_\epsilon$  (the solution may be analytic in some cases, see section IV);

- the scale factor  $\varepsilon$ .

The corresponding relation is given close to the corner by:

$$E_\varepsilon(r, \theta) = \lambda \varepsilon^{(\alpha-1)} E_\infty(r_\infty, \theta). \quad (7)$$

For instance, if the statistical distribution of the curvature radii is known for a series of  $N$  pieces used in a high-voltage device, it will be possible to compute the statistical distribution corresponding to the maximal electric field in these pieces.

### III. COMPUTATION OF THE SINGULARITY FACTOR

#### A. The Fourier method: weighted line integral of $v$

The Fourier method enables to compute an approximation of the singularity factor  $\lambda$  from the solution  $v$  of the problem with the sharp corner (see Fig. 1(b)) given by the FEM. A weighted integral of  $v$  is computed on an arc of circle of radius  $r_0$  centered on  $O$ , from one border of the angle to the other:

$$\lambda = \frac{2}{\omega} r_0^{-\alpha} \int_0^\omega v(r_0, \theta) \sin(\alpha\theta) d\theta. \quad (8)$$

When  $\theta$  varies between 0 and  $\omega$ ,  $\alpha\theta$  varies between 0 and  $\pi$ ; in this range of variation, the integration of  $\sin(\alpha\theta)$  with  $\sin(k\alpha\theta)$  is zero for all  $k$  strictly greater than 1. Relation (8) is then obtained by considering expansion (1) in the line integral.

There is no restriction in the choice of  $r_0$  except that the arc of circle must belong to the domain  $\Omega$ .

#### B. Dual solution method

The theoretical explanations concerning this method can be found in [1, Subsubsection 2.3.8]. This approach enables to compute the singularity factor  $\lambda$  from an integral on the domain  $\Omega$  with the sharp angle (see Fig. 1(b)) of a function  $v^*$  to compute, weighted by a function  $f$  which is the laplacian of a “regular lifting” function  $w$ :

$$\lambda = \int_\Omega f v^* ds. \quad (9)$$

It is proposed here not to construct this regular lifting but the less regular lifting which is commonly (but often implicitly) used in the FEM. It is shown that this FEM lifting can be used in the same manner but first, a few elements are given to understand where this expression comes from.

Our explanations take place on a domain  $\Omega_\delta$ , see Fig. 2. It can be seen that when the radius  $\delta$  of the circle  $C_\delta$  goes to zero,  $\Omega_\delta$  converges to  $\Omega$ , see Fig. 1(b).

For two functions  $v$  and  $v^*$  of zero laplacian in  $\Omega_\delta$ , it can be written:

$$0 = \int_{\partial\Omega_\delta} \left( \frac{\partial v}{\partial \mathbf{n}} v^* - v \frac{\partial v^*}{\partial \mathbf{n}} \right) dl, \quad (10)$$

where  $\mathbf{n}$  is the unitary outward normal on the boundary of the domain. As in [1], integral (10) can be made explicit on each boundary of the domain for a non zero  $\delta$  and then take the limit when  $\delta$  goes to zero, by considering the particular properties of the functions  $v$  and  $v^*$ .

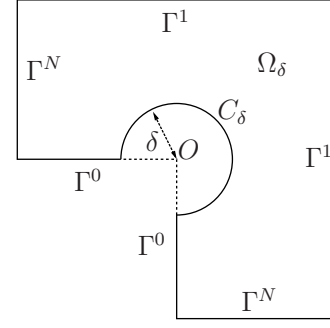


Fig. 2. Domain  $\Omega_\delta$  where  $\delta \rightarrow 0$  is considered.

In this computation,  $v$  is the FEM solution of the problem on  $\Omega$  detailed in Subsection II-A. The function  $v^*$  is the same as in [1]. It is the sum of the “dual singular function”  $S^*$ :

$$S^*(r, \theta) = r^{-\alpha} \sin(\alpha\theta), \quad (11)$$

and a more regular function  $v_R^*$  computed on the domain  $\Omega$  which is the solution of the following problem:

$$\begin{cases} \Delta v_R^* = 0, & \text{on } \Omega, \\ v_R^* = -S^*, & \text{on } \Gamma^0 \cup \Gamma^1, \\ \frac{\partial v_R^*}{\partial \mathbf{n}} = -\frac{\partial S^*}{\partial \mathbf{n}}, & \text{on } \Gamma^N. \end{cases} \quad (12)$$

Problem (12) can be solved by the FEM. Thus it is obtained:

$$v^* = v_R^* + S^*, \quad (13)$$

which is a singular non zero function. Moreover  $v^*$  has the following properties:

$$\begin{cases} \Delta v^* = 0, & \text{on } \Omega, \\ v^* = 0, & \text{on } \Gamma^0 \cup \Gamma^1, \\ \frac{\partial v^*}{\partial \mathbf{n}} = 0, & \text{on } \Gamma^N. \end{cases} \quad (14)$$

Considering again the path integral (10) when  $\delta$  goes to zero, the integrations are restricted to  $\Gamma^1$  and  $C_\delta$ :

$$\begin{aligned} 0 &= \lim_{\delta \rightarrow 0} \int_{\partial\Omega_\delta} \left( \frac{\partial v}{\partial \mathbf{n}} v^* - v \frac{\partial v^*}{\partial \mathbf{n}} \right) dl, \\ &= \lim_{\delta \rightarrow 0} \int_{\Gamma^1} -v \frac{\partial v^*}{\partial \mathbf{n}} dl + \lim_{\delta \rightarrow 0} \int_{C_\delta} \left( \frac{\partial v}{\partial \mathbf{n}} v^* - v \frac{\partial v^*}{\partial \mathbf{n}} \right) dl. \end{aligned} \quad (15)$$

It can be shown that the path integral on  $C_\delta$  converges to  $\pi\lambda$  when  $\delta$  goes to zero ( $\lambda$  being the sought singular factor):

$$\lim_{\delta \rightarrow 0} \int_{C_\delta} \left( \frac{\partial v}{\partial \mathbf{n}} v^* - v \frac{\partial v^*}{\partial \mathbf{n}} \right) dl = \pi\lambda. \quad (16)$$

Moreover, the integral on  $\Gamma^1$  in (15) can be written:

$$\int_{\Gamma^1} -v \frac{\partial v^*}{\partial \mathbf{n}} dl = -V^1 \int_{\Gamma^1} \frac{\partial v^*}{\partial \mathbf{n}} dl. \quad (17)$$

It is an integral only on the boundaries with non zero Dirichlet conditions (that are far from the corner), and it corresponds to the flux on each of these boundaries of the dual solution  $v^*$ .

This is a “classical” computation in the FEM, that can be done by a *surface* integral, on a transition layer  $\text{CT}^1$  (often limited to one layer of elements in direct contact with the boundary), of the scalar product of the gradients of the functions  $v^*$  and  $V^1 w$ , where  $w$  is equal to 1 on  $\Gamma^1$  and goes to zero through the layer:

$$-V^1 \int_{\Gamma^1} \frac{\partial v^*}{\partial \mathbf{n}} dl \approx V^1 \int_{\text{CT}^1} \nabla w \cdot \nabla v^* ds. \quad (18)$$

In fact,  $V^1 w$  is the FEM lifting and it can be seen as an application of (9), by taking the laplacian of  $V^1 w$  as a distribution. Eventually, the singularity factor is given by:

$$\lambda = -\frac{1}{\pi} V^1 \int_{\text{CT}^1} \nabla w \cdot \nabla v^* ds. \quad (19)$$

### C. Numerical comparison of both methods

The singularity factor  $\lambda$  is computed on a geometry similar to this on Fig. 1(b), where the length of each straight part of  $\Gamma^0$  is equal to 50 mm, the length of each straight part of  $\Gamma^N$  is equal to 50 mm and finally the length of each straight part of  $\Gamma^1$  is equal to 100 mm. The boundary conditions are also the same as these described in Subsection II-A. The potential  $V^1$  is chosen equal to 1.

It is shown on Fig. 3 that for the method proposed in Subsection III-A, the computed result for  $\lambda$  is dependent on the choice of  $r_0$ . As  $r_0$  increases, the computed value for  $\lambda$  quickly coincides for both methods.

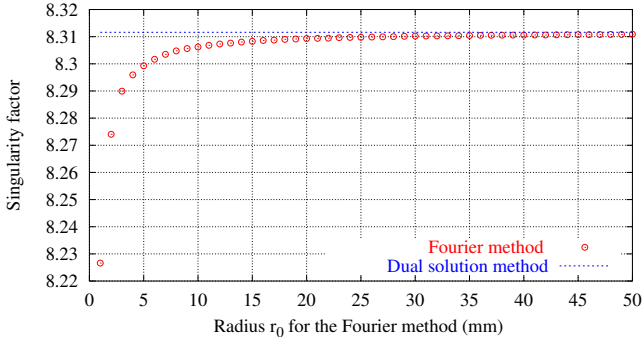


Fig. 3. Value of  $\lambda$  computed by the method described in Subsection III-A as a function of  $r_0$ . The dotted line indicates the value computed by the method described in Subsection III-B.

## IV. SOLUTION OF THE PROBLEM IN $\Omega_\infty$

It was introduced in Subsection II-A a potential  $v_\infty$  solution of the Laplace equation on the unbounded domain  $\Omega_\infty$ .

In Subsection IV-A, the problem for  $v_\infty$  is formulated as a classical Laplace problem with non homogeneous boundary conditions, straightforwardly solved by the FEM. In Subsection IV-B, it is shown that conformal maps may give a solution for certain specific shapes of the rounded corner. In Subsection IV-C, the practical method used to obtain the approximation (6) by combining the solution  $v_\infty$  with the solution  $v$  on the domain with the sharp corner, is explained.

### A. The equivalent problem with shifted singularity

Let us define a new function  $S_\infty$ , with the correct behavior at infinity (3) and whose laplacian is zero in  $\Omega_\infty$ . Note that  $S$  itself is not suitable, because its laplacian is not defined in  $O$  ( $r$  equal to 0). We propose for instance:

$$S_\infty(r, \theta) = r_s^\alpha \sin(\alpha\theta), \quad (20)$$

where  $r_s$  is the distance between the observation point and any point inside the infinite conductor, typically the center of curvature of the rounded corner (Fig. 4).

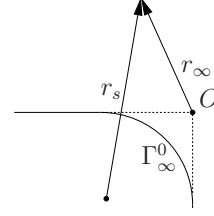


Fig. 4. Definition of  $r_s$

The behavior at infinite is obviously correct, but this function is not zero on the surface of the conductor:  $v_\infty$  will be written as the sum of this function  $S_\infty$  and a corrective potential  $v_{R\infty s}$ :

$$v_\infty = S_\infty + v_{R\infty s} \quad (21)$$

which is the solution of:

$$\begin{cases} \Delta v_{R\infty s} = 0, & \text{on } \Omega_\infty, \\ v_{R\infty s} = -S_\infty, & \text{on } \Gamma_\infty^0, \\ \lim_{r_\infty \rightarrow \infty} v_{R\infty s}(r_\infty, \theta) = 0. \end{cases} \quad (22)$$

This regular potential  $v_{R\infty s}$  can be found with the FEM and a classical “shell transformation” for taking into account the unbounded domain [6]. Then,  $v_\infty$  is obtained by (21).

### B. Method of conformal maps

The method of conformal maps [7] allows to build analytically potentials with the properties requested for  $v_\infty$ , i.e. equal to zero on the conductor and with a prescribed behavior at infinity, on domains like  $\Omega_\infty$ . However, only some particular shapes are reachable by these transformations.

1) *Example of transformation for a rounded corner:* Let us consider the two complex planes:

$$z = x + iy = re^{i\theta} \text{ corresponding to the real geometry,} \quad (23)$$

$$w = u + iv = Re^{i\phi} \text{ where } v \text{ is the electric potential.} \quad (24)$$

and the following conformal map [8, p. 320]:

$$z = k[(w + a)^{1/\alpha} + (w - a)^{1/\alpha}], \quad (25)$$

with  $a = 2^{\alpha-1}$  and  $k = 1/2$ .

The image of the straight line  $v = 0$  in the  $w$ -plane is composed of (see Fig. 5):

- the half-line  $y = 0$ ,  $x > 1$ , for  $u > a$  ( $u - a > 0$  and  $u + a > 0$ );

- the half-line  $re^{i\pi/\alpha}$ ,  $r > 1$ , for  $u < -a$  ( $u - a < 0$  and  $u + a < 0$ );
- a rounded line from  $P_l(z_l = e^{i\pi/\alpha})$  to  $P_r(z_r = 1)$ , for  $u \in [-a, a]$ , ( $u - a < 0$  and  $u + a > 0$ ).

Moreover, for  $|w| \gg |a|$ ,  $z \approx w^{1/\alpha}$  and  $v = \Im(w) = R \sin(\phi) \approx r^\alpha \sin(\alpha\theta)$ , what is the expected behavior at infinity. Then, this transformation gives the solution  $v_\infty$  for the particular shape given by (25).

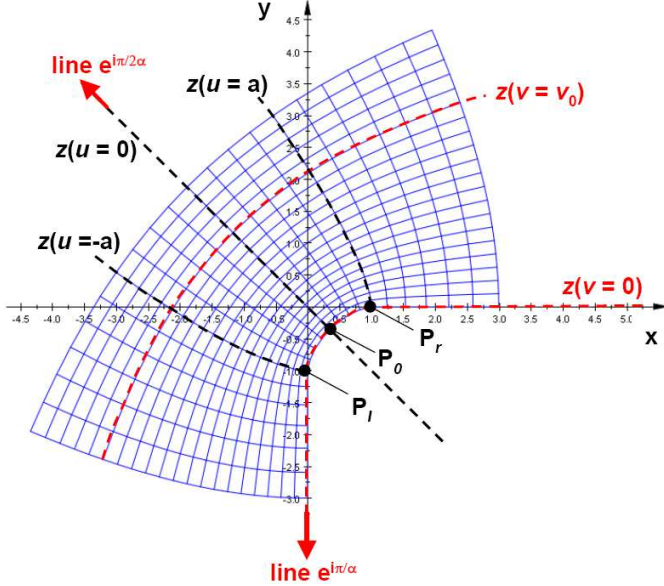


Fig. 5.  $z(u = \text{constant})$  and  $z(v = \text{constant})$  plotted in the  $z$ -plane for the conformal map (25)

2) *Reference values of the electric field:* The electric field on the conductor, for any point on the right of the rounded corner ( $v = 0$ ,  $u > a$ ) is:

$$-\frac{dv}{dy} = \frac{-2\alpha}{(u+a)^{(1-\alpha)/\alpha} + (u-a)^{(1-\alpha)/\alpha}}. \quad (26)$$

For example, the modulus values of  $E_\infty$  are:

$$|E_\infty(P_l)| = |E_\infty(P_r)| = \alpha 2^\alpha, \quad (27)$$

at the ends of the rounded corner, and:

$$|E_\infty(P_0)| = \frac{\alpha 2^{(1-\alpha)^2/\alpha}}{\sin\left(\frac{\pi}{2\alpha}\right)}, \quad (28)$$

on the middle-point of the rounded corner.

For the right angle ( $\alpha = 2/3$ ), the field is constant on the rounded corner:

$$|E_\infty(\alpha = 2/3, \varepsilon = 1)| = 2^{5/3}/3 = 1,058267... \quad (29)$$

even though it varies for other values of the conducting corner.

The approximate field on the real structure at the same points is deduced from  $E_\infty$  using (7): for this computation, only the scale  $\varepsilon$  and the singularity factor  $\lambda$  are required.

We propose to use the reference field (28), or its particular value 1.06 for a right rounded angle, when the shape of the rounding is not exactly known, and when an approximation of

the maximum field as function of the mean curvature of the corner is the requested information.

3) *Remarks:* Such conformal maps have the required behavior (at infinite and on the straight parts of the conductor) for favorably replacing the shifted singular function  $S_\infty$ , (20) used in Subsection IV-A: the condition is that the line  $v = 0$  remains inside the real conductor (at the reference scale  $\varepsilon = 1$ ). By the way, the norm of the correction  $v_{R\infty s}$  (22) will probably be reduced.

### C. Scaling by $\varepsilon$ : projection method

Whatever the method used to build  $v_\infty$  in the domain  $\Omega_\infty$  (the FEM, conformal maps or another method), this potential is not directly constructed in the mesh where  $v$  is computed on the domain  $\Omega$  with the sharp angle.

Moreover, the computation of the sum (5) and (6) for a particular  $\varepsilon$ , on a domain  $\Omega_\varepsilon$ , see Fig. 1(a), requires a projection of  $v_\infty$  on the mesh of the final domain, with a scaling factor different for each value of  $\varepsilon$ . For this purpose, the projection is performed by a continuous least-square approach [9].

When only the results in some particular points is of interest, such as the amplitude of the electric field in the middle of the rounded corner, this step requires no particular computation.

### D. Numerical results

It is considered the same problem as in Subsection III-C.

It is shown on Fig. 6, the good agreement between results obtained by formula (7) and results obtained by straightforward FEM computations. In order to plot these results, the solution  $v_\infty$  is computed by considering the method proposed in Subsection IV-A and  $\lambda$  is computed by the method proposed in Subsection III-B. To be precise, the values retained for  $\max(|E_\infty|)$  and for  $\lambda$  are respectively 1.1467 V/m and 8.31235 (the value for  $\max(|E_\infty|)$  can be compared to the value 1.06 V/m that is given by the conformal map described in Subsection IV-B).

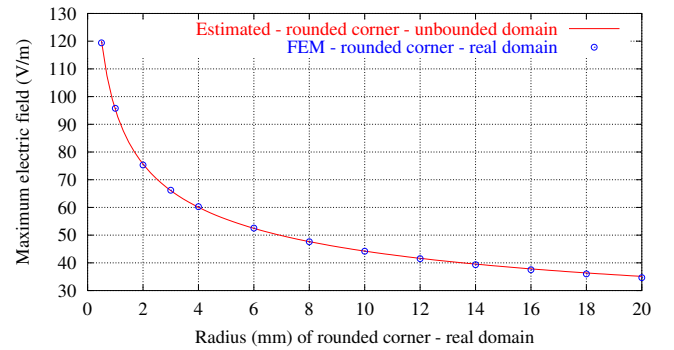


Fig. 6. Comparison of the maximum electric field on the rounded corner between results obtained by straightforward FEM computations and results obtained by relation (7).

It is also shown on Fig. 7 that the knowledge of  $\lambda$  and  $v_\infty$  provides an accurate approximation of the normal electric field on the conductor close to the corner (relation (5)) and that  $v$  and relation (6) provide accurate approximations of the normal electric field on the conductor far from the corner.

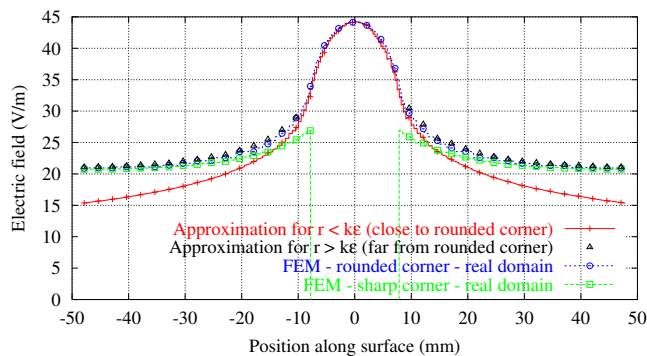


Fig. 7. Comparison of the normal electric field on the conductor for  $\varepsilon = 10$  mm.

## V. CONCLUSION AND PERSPECTIVES

In this work, a set of practical techniques was proposed to enable the implementation of new methods to estimate the electric field in the neighborhood of conductors containing rounded angles, in the 2D case.

The computation on the whole studied structure can be done by replacing rounded corners by sharp corners. A generic auto-similar solution enables to estimate the electric field close to the corner by post-processing for several values of the curvature radius. Some numerical tests have assessed the relevance of the proposed approach.

It has been also shown that forgotten techniques, as conformal maps, enable, in some cases, to build exactly the generic solution and in every case, to approximate it. They can be coupled with more computationally intensive numerical methods as the FEM, by providing speed and accuracy.

We are currently working to the extension of these techniques to:

- cases with several angles (such as some MEMs applications),
- 3D cases which is our real aim,
- singularity treatment (with sharp corners) for eddy-current problems, that lead also to self-similar solutions, with the penetration depth  $\delta$  playing the same role as the scaling factor  $\varepsilon$  in the present study.

## REFERENCES

- [1] H. Timouyas, "Analyse et analyse numérique des singularités en électromagnétisme," Ph.D. dissertation, Ecole Centrale de Lyon, 2003. [Online]. Available: <http://tel.archives-ouvertes.fr/tel-00110828>.
- [2] M. Dauge, S. Tordeux, and G. Vial, *Around the Research of Vladimir Maz'ya II: Partial Differential Equations*. Springer Verlag, 2010, ch. Selfsimilar Perturbation near a Corner: Matching Versus Multiscale Expansions for a Model Problem, pp. 95–134.
- [3] L. Krähenbühl, H. Timouyas, M. Moussaoui, and F. Buret, "Coins et arrondis en éléments finis - Une approche mathématique des coins et arrondis pour les solutions par éléments finis de l'équation de Laplace," *RIGE*, vol. 8, pp. 35–45, 2005.
- [4] S. Tordeux, G. Vial, and M. Dauge, "Matching and multiscale expansions for a model singular perturbation problem," *Comptes Rendus Mathématique*, vol. 343, no. 10, pp. 637–642, Nov. 2006.
- [5] P. Grisvard, *Elliptic problems in nonsmooth domains*. Pitman Advanced Pub. Program, 1985.

- [6] F. Henrotte, B. Meys, H. Hedia, P. Dular, and W. Legros, "Finite element modelling with transformation techniques," *Magnetics, IEEE Transactions on*, vol. 35, no. 3, pp. 1434–1437, 1999.
- [7] Wikipedia. Conformal map. [Online]. Available: [http://en.wikipedia.org/wiki/Conformal\\_map](http://en.wikipedia.org/wiki/Conformal_map)
- [8] E. Durand, *Electrostatique, Vol. 2 : Problèmes généraux conducteurs*. Editions Masson, Paris, 1964-1966.
- [9] C. Geuzaine, B. Meys, F. Henrotte, P. Dular, and W. Legros, "A Galerkin projection method for mixed finite elements," *Magnetics, IEEE Transactions on*, vol. 35, no. 3, pp. 1438–1441, 1999.